MECHANIKA TEORETYCZNA
I STOSOWANA
Journal of Theoretical
and Applied Mechanics
2, 34, 1996

GENERATION OF FLOW PERIODICITY IN A WIND-TUNNEL EXPERIMENT

MARIAN WYSOCKI

STANISŁAW DROBNIAK

WITOLD ELSNER

Thermal Machinery Institute, Technical University of Częstochowa

e-mail: ppam@d.polczest.us.edu.pl

The paper presents an experimental analysis of the unsteady velocity field generated by the Periodic Flow Generator (PFG) installed at the wind-tunnel. The measurements were performed for two different designs of PFG which consisted of a row of either cylindrical bars or symmetric profiles. It was found that the wakes generated by the PFG with cylindrical bars were substantially distorted by Karman vortices. The reason responsible for this distortion was the fact that the Karman vortices appeared to be somewhat synchronized with the cylinder-wakes. The PFG built of symmetric profiles proved in turn to be an effective tool for generating the flow unsteadiness which, to some extend, could simulate the flow periodicity encountered at the inlet to the real axial-flow turbine stage.

It was also proved that this periodicity hardly changed the mean flow pattern behind the cascade of turbine blade, but, on the other hand, significantly modified the distributions of both the random and periodic flow disturbances.

Notation

b	–	chord length
c	–	absolute velocity
c_*	–	total time dependent velocity component, $c_* = c' + \tilde{c}$
$c', \tilde{c}$	–	random and periodic velocity fluctuation
d	–	PFG cylinder diameter
f	–	frequency

N	–	overall number of the periods recorded
Re	–	Reynolds number, $\mathrm{Re}_1 = \bar{c}_1 b_c / v_1$
St	–	Strouhal number, $\mathrm{St} = f_g d / w$
t_g	–	blade (profile) spacing
t_c	–	blade (cascade) spacing
u	–	velocity of PFG disturbing elements
w	–	relative velocity
Δ	–	difference
τ	–	nondimensional time scale
$(\bar{\cdot})$	–	time mean value
$\langle(\cdot)\rangle$	–	phase-averaged value
(x, y, z)	–	spatially fixed coordinate systems.

1. Introduction

Turbomachinery flow-fields are difficult to theoretical approach because they are highly unsteady, turbulent, three-dimensional and spatially non-homogeneous. For this reason, much of the insight into the complex physical mechanisms that govern a turbomachinery aerodynamics has come from a broad range of experimental studies utilizing fast response instrumentation. A lot of these works were done in linear or annular cascades installed in conventional wind-tunnels, which did not allow, however, the unsteady flow phenomena that occur in a real turbomachinery to be studied. So, there appeared an urgent need in the cascade research to raise the possibility to generate a periodically varying flow field, which to some extent could represent the flow-pattern existing in a real turbomachinery stage. One of the first attempts in this domain was made by Satyanarayana (1977) who conducted his research in a specially designed gust-tunnel at Cambridge University where the sinusoidal gusts were generated in a wind-tunnel measuring section.

Another example of periodic flow stimulation was described by Adachi and Murakami (1979) who applied a rotor wheel with two cylindrical bars to simulate in an annular wind-tunnel the reaction of the real rotor blades.

An interesting experimental analysis of the unsteady three-dimensional flow and pressure field in an annular compressor cascade was carried out by Schulz and Gallus (1990) and later by Poensgen and Gallus (1991). Flow periodicity was generated by an upstream rotor which consisted of 24 cylindrical

rods, simulating rotor blades. Periodic flow unsteadiness in a wind-tunnel was also generated by Dullenkopf et al (1992), who installed a wake-generator at the tunnel exit, just before the test cascade. This generator consisted of a disc with cylindrical bars and its rotation was supposed to simulate the effect of rotor blades.

Following that way, at the Technical University of Częstochowa a pulse flow generator of a discontinuous action has been build and tested. The aerodynamic performance of this facility designed to produce an inflow periodicity in wind-tunnel research is the main subject of the present report.

2. Experimental facility and apparatus

The main part of the Periodic Flow Generator, thereafter referred to as PFG, represents an array consisting alternatively of cylindrical bars or symmetrical profiles suitably angled with respect to the initial velocity direction, as shown in Fig.1.

The PFG has been installed at the wind-tunnel exit just before a linear cascade of turbine stator profiles. Assuming the Reynolds number $\mathrm{Re}_1 = c_1 \cdot b_c/v = 2 \cdot 7 \cdot 10^5$ and the velocity ratio $u/c_1 = 0.5$ one can find $u = 6.7\,\mathrm{m/s}$ as a PFG velocity. The spacing t_g of the PFG's profile has been fixed as $t_g = 80\,\mathrm{mm}$ that corresponds to the typical axial turbine stage with $t_c/t_g = 3$.

The unsteady flow behaviour has been analysed using a two-channel DISA 55M System hot-wire anemometer coupled with a PC computer. In order to analyse the periodic flow unsteadiness it has been found necessary to apply the phase lock averaging procedure, utilizing the reference signal taken from the position sensor of the PFG. During the measurements of the Karman-vortex street behind the motionless PFG's profiles the 3567A Hewlett-Packard analyser has also been utilized. More details of the experimental facility and data processing applied in the experiment described are given by Wysocki (1995).

3. Flow field pattern produced by PFG with cylindrical rods

A first step in this stage of experiment was to determine the necessary number of periods recorded at a given point of the flow field, which, taken

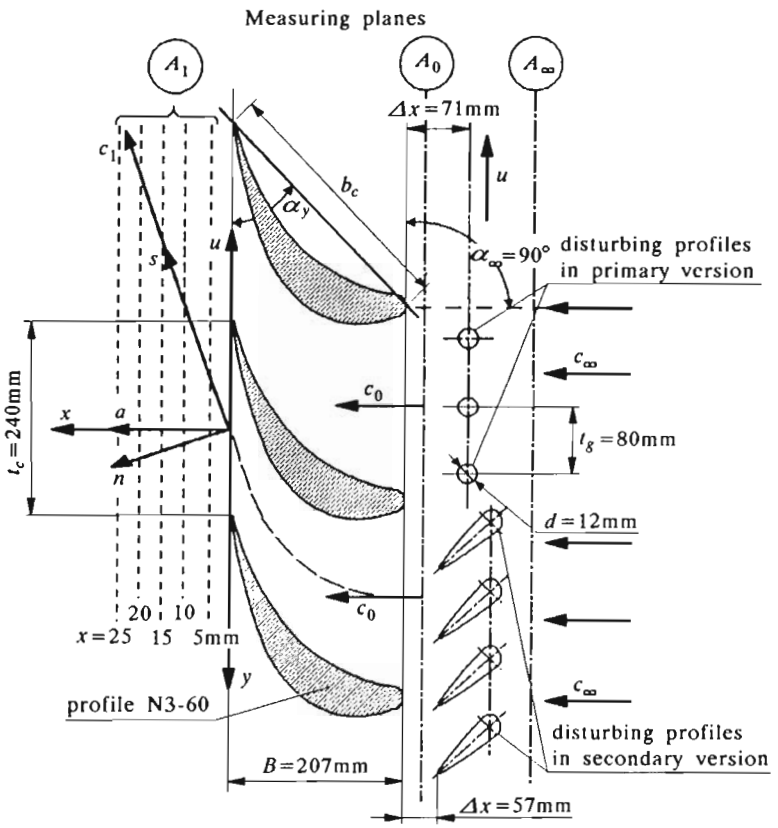

Fig. 1. The parameters of cascade and PFG and their mutual location

into account in the phase-averaging procedure, could ensure a constant value of a periodic velocity variance $\overline{\tilde{c}^2}$ and a stable shape of a phase-averaged velocity profile $\langle c(\tau)\rangle$. In order to answer this question a single hot-sensor was placed in a fixed point behind the PFG, with its wire normal to the xy plane (see Fig.1). A sample velocity – time record, together with a reference signal is presented in Fig.2. As may be seen, the function $c(t)$ does not exhibit any trace of a periodic character and this observation is additionally confirmed by the data plotted in Fig.3. The value of the overall velocity variance $\overline{c_*^2} = \overline{\tilde{c}^2} + \overline{c'^2}$ attains a constant value at $N = 40$ recorded periods, while the periodic variance $\overline{\tilde{c}^2}$ appears to be a monotonic decreasing function of the N number. At the same time the shape of a phase averaged velocity profile $\langle c(t)\rangle$ (not shown here) tends to a practically constant value without any symptoms of flow periodicity.

Fig. 2. The sample record of a reference signal (a) and velocity signal (b)

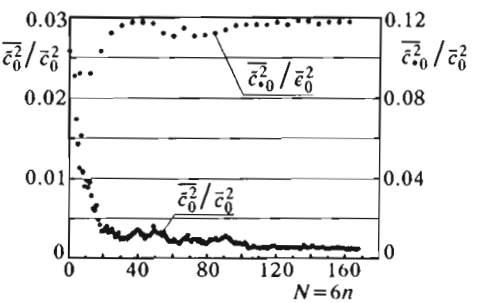

Fig. 3. The distribution of overall and periodic velocity variance

The observed phenomenon may be probably explained by the fact, that the viscous wakes appearing periodically in a flow-field with a frequency $f_g = U/t_g$ are distorted by the Karman vortices shed from the moving cylinders with the frequency f_k, resulting from the unanimously accepted Strouhal number

$$\mathrm{St} = f_k \frac{d}{\sqrt{c^2 + u^2}} \simeq 0.2$$

In order to get a better insight into this problem it was decided to examine the flow characteristics behind a row of motionless cylinders. The distributions of mean as well as fluctuating velocities normalized by the spatially averaged value, $(\overline{c_0})_{avr}$ have been presented in Fig.4 for one arbitrarily chosen value $x/d = 4.2, (x/t_g = 0.625)$. The measurements which embraced three cylinder spacings $(-1.5 < y/t_g < 1.5)$ have shown an evident spatial repeatability of both the curves plotted there.

In order to determine the extent of a Karman vortex street a spectral

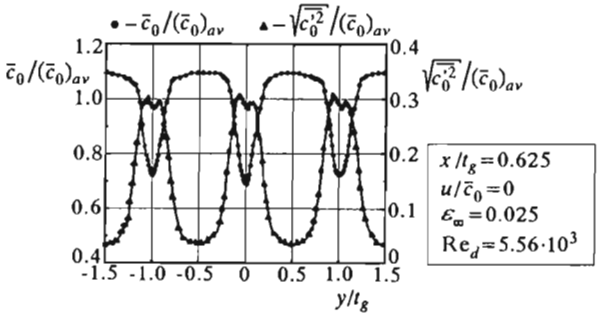

Fig. 4. The distribution of normalized mean and fluctuating velocities behind stationary cylindrical bars

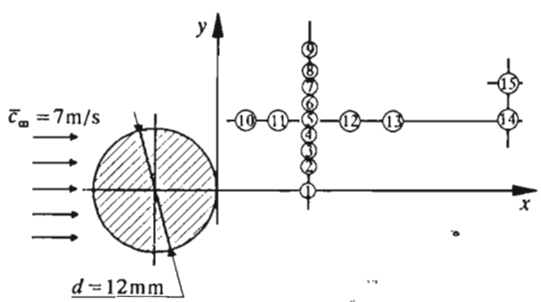

Fig. 5. The scheme of measuring points location behind a motionless cylinder

analysis of hot-wire signals behind the middle cylinder has been performed according to the scheme given in Fig.5. Traversing the probe in $x/d = 2.3$ plane, a maximum of a hot-wire spectral response has been found at a point 5 ($y/d = 0.58$) with a peak at the Karman vortex frequency (see Fig.6) corresponding to the Strouhal number $St = f_k d/\overline{c_\infty} = 0.19$, being in agreement with the findings of other authors, e.g., Wierciński (1989).

In the next step the hot-sensor has been traversed along the line $y/d = 0.58$. The obtained results, rearranged in the form explained in Fig.7, have shown that in the further flow region, say $x/d > 8$, the function $\Delta A(x/d)$ considerably decreases what must have been attributed to the decay of organized vorticity in a Karman vortex street. The velocity-time record taken at point 5 and presented in Fig.8 confirms an existence of periodic velocity component with significant amplitude $(\tilde{c})_{max}/\bar{c} \simeq 1$. Because the frequencies f_g and f_k of both the periodic phenomena simultaneously existing in the flow

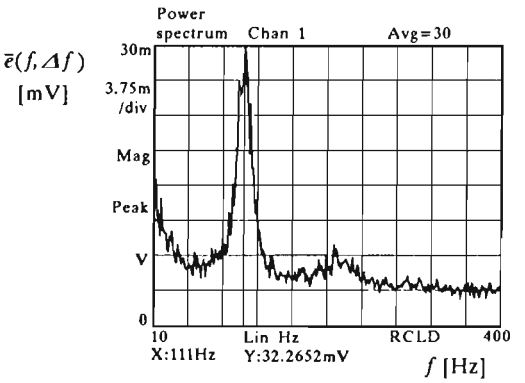

Fig. 6. The amplitude spectrum of hot-wire voltage in a wake behind a motionless cylinder

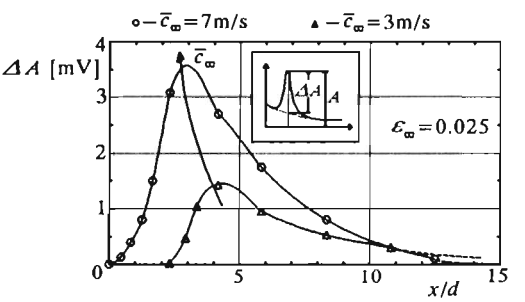

Fig. 7. The zone of Karman vortex apperance determined from amplitude spectra

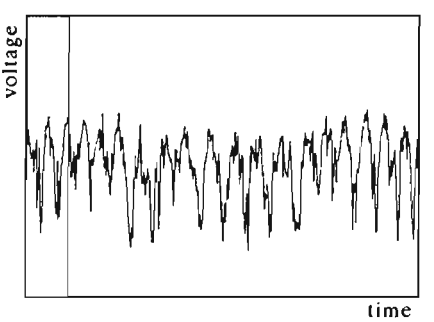

Fig. 8. The velocity-time record taken at point No.5 behind a stationary cylinder

considered are mutually intercorrelated according to the relation

$$\frac{f_g}{f_k} = \frac{d}{t_g \mathrm{St}} \frac{1}{\sqrt{1+\varphi^2}} \qquad \left(\varphi = \frac{c}{u}\right)$$

so, in some flow situations, the Karman vortices may destroy the expected regularity of the viscous wakes generated by the moving cylinders. That is probably the reason why the attempts to produce flow periodicity by means of a moving row of cylinders have ended in failure. The more detailed inspection of the problem, though in a slightly different type of flow, has been undertaken by Bogusławski and Elsner (1994).

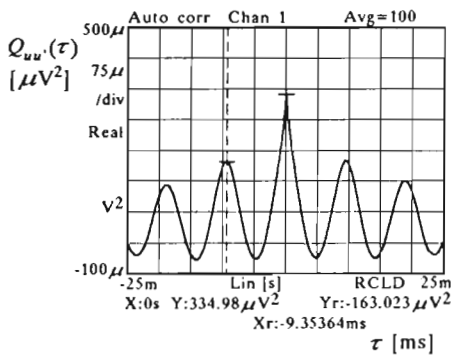

Fig. 9. The autocorrelation function $Q_{uu}(\tau)$ of the velocity behind the motionless cylinder

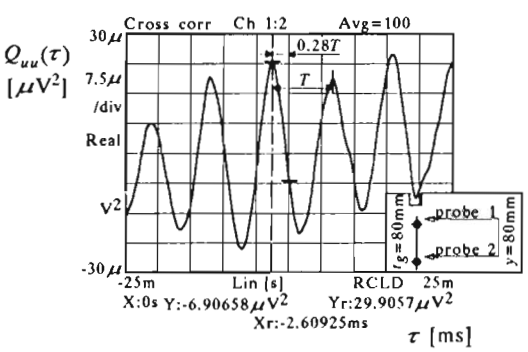

Fig. 10. The cross-correlation function $Q_{uu'}(\tau)$ of the velocity u and u'

In the same experiment concerning the row of motionless cylinders another interesting observation was taken. The autocorrelation function of velocity $Q_{uu}(\tau)$ taken at point 5 and presented in Fig.9, has a clear periodic form.

The period of this function $T = 1/f_k$ corresponds, as it was supposed, to the frequency of Karman vortex shedding. The same periodicity has also been found in the cross-correlation $Q_{uu'}(\tau)$ function (see Fig.10) of the velocity signals $u(t)$ and $u'(t)$ originating from two hot-wire probes set with the distance equal to blade spacing t_g. As it can bee seen, the middle peak of this function is shifted at about 28% of period T relative to $\tau = 0$ correlation time. This observation allowed conclusion that, in spite of numerous opinions (presented e.g. by Wierciński (1989), the shedding of the vortices from two neighboring cylinders takes place not in opposite phase but it is rather separated by the $T/4$ phase delay.

4. Flow characteristics behind the PFG with a row of symmetrical profiles

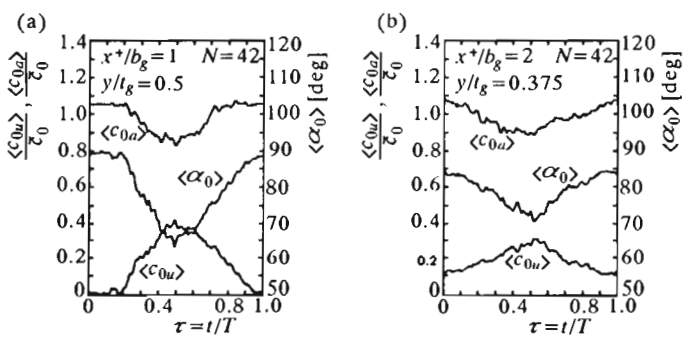

Fig. 11. The sample distribution of axial and tangential velocity components as well as flow angle variation for $x/b_g = 1$ (a) and $x/b_g = 2$ (b); $\varepsilon_\infty = 0.025$, $\mathrm{Re}_{b_g} = 2.05 \cdot 10^4$

Because of the difficulties encountered with the use of cylindrical bars as the disturbing elements of the PFG, they have been replaced by a row of symmetrical profiles showing only slight trace of the Karman vortices. An analysis of the oscillating velocity field behind the PFG was performed with the DISA 55P61 X-probe, giving both the axial $\langle c_u(\tau)\rangle$ and tangential $\langle c_u(\tau)\rangle$ phase-averaged velocity components in z=constant plane. Their normalized profiles as well as flow angle variations $\langle \alpha(\tau)\rangle$ determined in two sample control planes $x/b_g = 1$ and 2 are presented in Fig.11. As can be seen, with an increase of x coordinate the amplitudes of $\langle c_u(\tau)\rangle$ variation decrease

evidently, and, at the same time, the non-zero value appears for $\tau = 0$ and 1, giving in consequence the drop in $\langle\alpha(\tau)\rangle$ angle for $\tau = 0$ and 1.

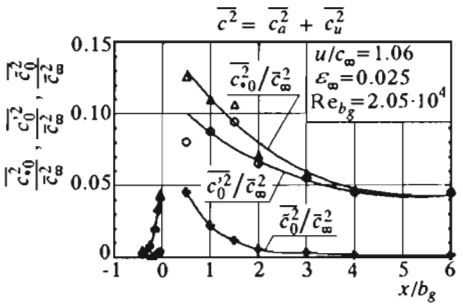

Fig. 12. Total, periodic and random velocity in front $(x/b_g < 0)$ and behind $(x/b_g > 0)$ the PFG

The decay of the total, $\overline{c_*^2}$ periodic $\overline{\tilde{c}^2}$ and random $\overline{c'^2}$ velocity variances is illustrated in Fig.12. As can be seen, the energy contained within the periodic fluctuations is much lower than the turbulent one.

5. Structure of velocity field behind the cascade in the presence of inflow periodic disturbances

An analysis of the flow field downstream of the test-cascade has been carried out in several control planes parallel to the stator trailing edges (see Fig.1). The measurements were realized for two cases, i.e., for the flow stimulated by the PFG consisting of an array of symmetrical profiles as well as for the undisturbed flow, which was treated as a reference level.

As can be seen in the sample plane $x/b_c = 0.0167$ (see Fig.13), located just behind the trailing edges of the particular profiles, the periodic stimulation of the inlet velocity field does not cause any substantial differences in the mean flow pattern behind the cascade except small discrepancies which may be noted in the wake regions.

The influence of the inlet flow periodicity becomes more clear if analysis is extended upon the random ε', periodic $\tilde{\varepsilon}$ and total ε_* intensities of velocity fluctuations, described here as

$$\varepsilon'(y/t_c) = \frac{\sqrt{\frac{1}{3}\left[\overline{c_i' c_i'}(y/t_c)\right]}}{\overline{c}(y/t_c)} \qquad \tilde{\varepsilon}(y/t_c) = \frac{\sqrt{\frac{1}{3}\left[\overline{\tilde{c}_i \tilde{c}_i}(y/t_c)\right]}}{\overline{c}(y/t_c)}$$

$$\varepsilon_*(y/t_c) = \frac{\sqrt{\frac{1}{3}\left[\overline{c_i'c_i'}(y/t_c) + \overline{\tilde{c}_i\tilde{c}_i}(y/t_c)\right]}}{\overline{c}(y/t_c)} \qquad i = s, n, z$$

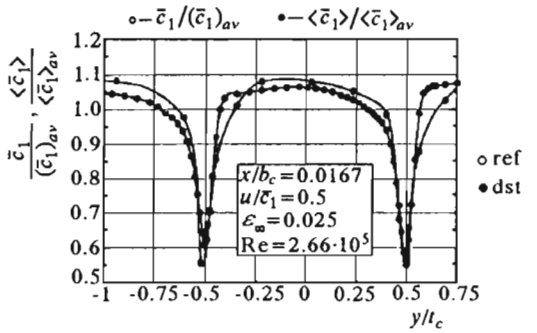

Fig. 13. Comparison of time-mean velocity profiles behind the cascade for the reference (circles) and disturbed flow (black points)

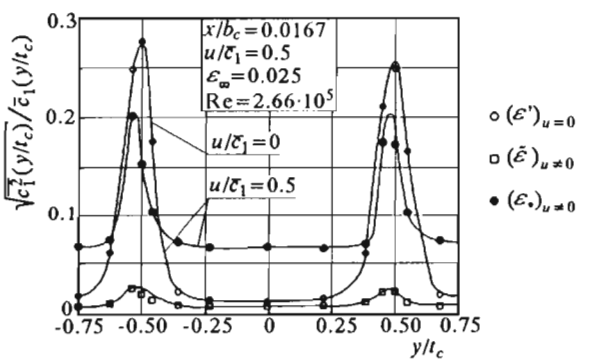

Fig. 14. Intensities of velocity fluctuations measured behind the cascade for reference and disturbed flow

The above intensities are plotted in Fig.14 for both the cases being compared i.e. for the stimulated ($u \neq 0$) as well as undisturbed flow ($u = 0$). As may be seen, the periodic intensity $\tilde{\varepsilon}_{u\neq 0}$ is clearly visible in the wake regions where, on the other hand, the total intensity $(\tilde{\varepsilon}_*)_{u\neq 0}$ drops below the level of $\varepsilon'_{u=0}$. Outside these regions intensity $(\tilde{\varepsilon}_*)_{u\neq 0}$ is much higher than $\varepsilon'_{u=0}$ and attains the value of about 7 percent.

Taking advantage of the hypothesis of uncorrelated random and periodic velocity fluctuations, we have

$$\overline{c_*^2} = \overline{\tilde{c}_i\tilde{c}_i} + \overline{c_i'c_i'}$$

hence

$$\frac{\overline{\widetilde{c}_i\widetilde{c}_i}}{\overline{c_*^2}} = 1 - \frac{\overline{c_i'c_i'}}{\overline{c_*^2}} \qquad i = s, n, z$$

The contribution, defined above, brought by the periodic motion into the total energy of velocity fluctuations and presented in Fig.15 for the $x/b_c = 0.0167$ cross-section, does not exceed 2 percent even in the wake regions. Bearing in mind the substantial modification of fluctuating velocity field introduced by the PFG action (see Fig.14) this surprisingly low contribution suggests the complex impact of periodic flow stimulation on the aerodynamics of the cascade blades. The above data confirm the affectiveness of the periodic flow stimulation applied in the present work while the more details of the flow structure around the blade may be found in the work by Elsner et al. (1995).

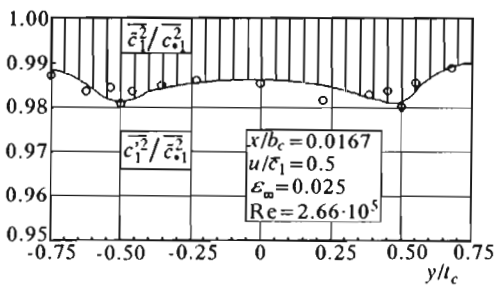

Fig. 15. Contributions of random and periodic motion to the total velocity variance behind the test-cascade

6. Conclusions

The results of the present experiment clearly show, that the PFG accompanied by the advanced measuring technique may be successfully used in a wind-tunnel experiment to produce a flow periodicity similar in a some measure to that, induced by the rotor blade row rotating in a real axial-flow turbine stage. In particular, it has been found that the PFG was able to generate the substantial inlet flow angle variation characterized by the amplitude exceeding 30 degrees.

The experimental data reveal, that the periodic inlet flow stimulation hardly changes the mean flow pattern at the cascade exit. The substantial influence is observed, however, with respect to the level of velocity fluctuations,

which being evidently lower in the wake regions attain much higher values outside these regions. The periodic velocity component in the flow behind the cascade is strongly damped, so that its contribution to the total energy of velocity fluctuations does not exceed 2 percent.

This work was sponsored by the State Committee for Scientific Research under grant KBN PB 781/T07/95/08 No. 7T07C05008 as well as under statutory funds BS-03-301/91 provided by the Institute of Thermal Machinery.

References

1. ADACHI T., MURAKAMI Y., 1979, Three-Dimensional Velocity Distribution Between Stator Blades and Unsteady Force on a Blade Due to Passing Wakes, *Bull. of JSME*, **22**, 170, 1074-1082

2. BOGUSŁAWSKI A., ELSNER J.W., 1994, Wake Structure and Vortex Path Behind the Moving Circular Cylinder, *J. of Theoretical and Applied Mechanics*, **32**, 4, 735-751

3. DULLENKOPF K., SCHULZ A., WITTIG S., 1992, Turbine Airfoil Heat Transfer under Simulated Wake Conditions, *Proc.Int. Symposium Heat Transfer in Turbomachinery*, Athens, 1-14

4. ELSNER J.W., WYSOCKI M., DROBNIAK S., Effects of Flow Periodicity on the Aerodynamic Characteristics of a Linear Turbine Cascade, *ZN IMP PAN* (in print)

5. POENSGEN C., GALLUS H.E., 1991, There Dimensional Wake Decay Inside of a Compressor Cascade and its Influence on the Downstream Unsteady Flow Field, Part I – Wake Decay Characteristics in the Flow Passage, *Trans. ASME, J.Turbomachinery*, **113**, 180-189

6. SATYANARAYANA B., 1977, Unsteady Wake Measurements of Airfoils and Cascades, *AIAA J.*, **15**, 5, 613-618

7. SCHULZ H.D., GALLUS H.E., LAKSHMINARAYANA B., 1990, Three-Dimensional Separated Flow Field in the Endwall Region of an Annular Compressor Cascade in the Presence of Rotor-Stator Interaction: Part I – Quasi-Steady Flow Field and Comparison With Steady – State Data, Part II – Unsteady Flow and Pressure Field, *Trans ASME, J. of Turbomachinery*, **112**, Oct., 669-678 (I), 679-690 (II)

8. WIERCIŃSKI Z., 1989, The Geometry of Vortex Path Behind the Moving Cylinders Palisade, *IMP PAN Internal Report*, 280/1164/89, 3-24

9. WYSOCKI M., 1995, The Aerodynamic Characteristcs of a Linear Turbine Cascade under the Influence of Periodic Disturbance of Inflow Velocity Profile, PhD Thesis, Technical University of Częstochowa

Eksperymentalna generacja okresowości przepływu w tunelu aerodynamicznym

Streszczenie

W pracy przedstawiono eksperymentalną analizę pola prędkości generowanego przez symulator zaburzeń okresowych zainstalowany na wylocie z tunelu aerodynamicznego. Przebadano dwie wersje konstrukcyjnego rozwiązania generatora, w którym najpierw zastosowano palisadę prętów cylindrycznych a następnie palisadę profili symetrycznych. Jak potwierdzają to uzyskane wyniki, ślady generowane za cylindrycznymi prętami były silnie zniekształcone wpływem pól prędkości indukowanych przez wiry ścieżki Karmana, które w tym przypadku wykazywały synchronizację ze śladami aerodynamicznymi poszczególnych prętów. Palisada symetrycznych profili okazała się natomiast efektywnym źródłem niestacjonarności przepływu, która zgodnie z wynikami pomiarów symulować może periodyczny charakter przepływu istniejący na wlocie do rzeczywistego stopnia turbinowego.

Wykazano również, że niestacjonarność ta ma tylko nieznaczny wpływ na pole prędkości średniej za turbinową palisadą łopatkową, w istotny natomiast sposób oddziaływuje, w tym obszarze, na rozkłady intensywności zarówno losowych jak i periodycznych zaburzeń przepływu.

Manuscript received July 6, 1995; accepted for print December 8, 1995